UC Davis
UC Davis Previously Published Works

Title

Arabidopsis MAP65-4 plays a role in phragmoplast microtubule organization and marks the cortical cell division site

Permalink

Journal

ISSN

Authors

Li, Haoge
Sun, Baojuan
Sasabe, Michiko
et al.

Publication Date

DOI

Peer reviewed

Arabidopsis MAP65-4 plays a role in phragmoplast microtubule organization and marks the cortical cell division site

Haoge Li[1,2]*, Baojuan Sun[2,3]*, Michiko Sasabe[4], Xingguang Deng[2,5], Yasunori Machida[6], Honghui Lin[5], Y-R. Julie Lee[2] and Bo Liu[2]

[1]College of Biological Science and Technology, Shenyang Agricultural University, Shenyang, Liaoning 110866, China; [2]Department of Plant Biology, University of California, Davis, CA 95616, USA; [3]Vegetable Research Institute, Guangdong Academy of Agricultural Sciences, Guangzhou, Guangdong 510640, China; [4]Department of Biology, Faculty of Agriculture and Life Science, Hirosaki University, 3 Bunkyo-cho, Hirosaki 036-8561, Japan; [5]Key Laboratory of Bio-resources & Eco-environment, College of Life Science, Sichuan University, Chengdu 610064, China; [6]Division of Biological Science, Graduate School of Science, Nagoya University, Chikusa-ku Nagoya 464-8602, Japan

Summary

- The evolutionarily conserved MAP65 family proteins bundle anti-parallel microtubules (MTs). In *Arabidopsis thaliana*, mutations in the *MAP65-3* gene lead to serious defects in MT organization in the phragmoplast and cause failures in cytokinesis. However, the functions of other *Arabidopsis* MAP65 isoforms are largely unknown.
- MAP65 functions were analyzed based on genetic interactions among different *map65* mutations. Live-cell imaging and immunolocalization experiments revealed dynamic activities of two closely related MAP65 proteins in dividing cells.
- The *map65-4* mutation caused synthetic lethality with *map65-3* although *map65-4* alone did not cause a noticeable phenotype. Furthermore, the introduction of an extra copy of the *MAP65-4* gene significantly suppressed defects in cytokinesis and seedling growth caused by *map65-3* because of restoring MT engagement in the spindle midzone. During mitosis, MAP65-4 first appeared at the preprophase band and persisted at the cortical division site afterwards. It was also concentrated on MTs in the spindle midzone and the phragmoplast. In the absence of MAP65-3, MAP65-4 exhibited greatly enhanced localization in the midzone of developing phragmoplast.
- Therefore, we have uncovered redundant but differential contributions of MAP65-3 and MAP65-4 to engaging and bundling anti-parallel MTs in the phragmoplast and disclosed a novel action of MAP65-4 at the cortical cell division site.

Introduction

Eukaryotic cells organize microtubules (MTs) into physiologically important arrays by employing functionally distinct MT-associated proteins or MAPs. Different MAPs interact with MTs differently; for example, some bind MTs uniformly along the filaments while others preferentially associate with plus or minus ends of MTs. In plant cells, MAP65 proteins are among the most abundant MAPs that are tightly associated with various arrays of cytoplasmic MTs (Hamada *et al.*, 2013). MAP65 was first isolated from cultured tobacco cells, and founded an evolutionarily conserved MAP65/Ase1 protein family including the fungal Ase1 (Anaphase Spindle Elongation 1), and mammalian PRC1 (Protein Regulating Cytokinesis 1) (Jiang & Sonobe, 1993; Guo *et al.*, 2009). These proteins form homodimers so that they can serve as MT-bundling factor by cross-linking anti-parallel MTs preferentially (Walczak & Shaw, 2010).

Unlike fungi in which MAP65/Ase1 is encoded by a single gene in one species, flowering plants have multiple MAP65 genes. For example, MAP65 isoforms are encoded by nine genes in *Arabidopsis thaliana* and 11 genes in the rice *Oryza sativa* (Smertenko *et al.*, 2008; Guo *et al.*, 2009). These isoforms differ from each other by harboring divergent sequences toward the C-termini of the polypeptides (Smertenko *et al.*, 2008). Although they commonly serve as MT-bundling factors, their different localization patterns, as revealed by antibody immunolocalization as well as fusions with the green fluorescent protein (GFP), suggest that they probably carry out different intracellular functions (Van Damme *et al.*, 2004; Smertenko *et al.*, 2008). Furthermore, the MAP65 genes often exhibit different expression patterns. For example, MAP65-1 and MAP65-2 are constitutively expressed in all examined cells but MAP65-3 is predominantly expressed during cell division (Caillaud *et al.*, 2008; Ho *et al.*, 2011; Lucas & Shaw, 2012).

In *A. thaliana*, MAP65-1 and MAP65-2 function redundantly in promoting axial growth of rapidly expanding cells but their

---

*These authors contributed equally to this work.

functions are dispensable because the double null mutant sustains vegetative and reproductive growth at levels comparable to the wild-type (Lucas *et al.*, 2011; Sasabe *et al.*, 2011). By contrast, the loss of MAP65-3 leads to severe cytokinesis defects, resulting in seriously dwarfed seedlings (Müller *et al.*, 2004). After anaphase onset, MAP65-3 first appears in the middle region of the central spindle and later becomes concentrated at the phragmoplast midzone (Müller *et al.*, 2004; Van Damme *et al.*, 2004; Smertenko *et al.*, 2008; Ho *et al.*, 2011). Its function in cross-linking anti-parallel MTs in the phragmoplast is critical for engaging the two half-phragmoplasts so that cell plate assembly can take place effectively (Ho *et al.*, 2011). Although MAP65-1 and MAP65-2 exhibit certain degrees of functional redundancy with MAP65-3 as demonstrated by enhanced phenotypes of double mutants of *map65-3* and *map65-1* or *map65-2*, MAP65-1 and MAP65-2 localize uniformly along phragmoplast MTs during cytokinesis when genomic fusions with the GFP-coding sequence are employed for localization tests (Sasabe *et al.*, 2011; Lucas & Shaw, 2012; Smekalova *et al.*, 2014). Hence, MAP65-1/MAP65-2 may play a synergistic role in promoting MT activities, that is stability, instead of by performing the MT-cross-linking function at the MT-overlapping region in the phragmoplast (Ho *et al.*, 2012).

In the *map65-3* null mutant, a significant proportion of cells still divide successfully although c. 40% of the cytokinesis events are aborted (Ho *et al.*, 2012). Therefore, we hypothesized that the critical function of MAP65-3 in cross-linking anti-parallel MTs perhaps was shared with other protein(s) that localized at the phragmoplast midzone as MAP65-3 in *A. thaliana*. MAP65-4 was found to be more closely related to MAP65-3 than other MAP65 isoforms in a phylogenetic analysis (Guo *et al.*, 2009). However, current knowledge on MAP65-4 often argues against it having a redundant function as with MAP65-3. First, MAP65-4 bundles parallel and anti-parallel MTs nonselectively *in vitro* (Fache *et al.*, 2010). By contrast, MAP65-3 exclusively cross-links anti-parallel MTs (Ho *et al.*, 2011). Furthermore, when MAP65-4 of Arabidopsis origin was expressed in tobacco BY-2 cells using a cDNA construct under the control of the viral 35S promoter, the MAP65-4-GFP fusion protein decorated kinetochore MT fibers in mitotic spindles but not the preprophase band (PPB), central spindle or phragmoplast (Van Damme *et al.*, 2004; Fache *et al.*, 2010). In cultured Arabidopsis cells, however, MAP65-4 was detected in the anaphase central spindle and the phragmoplast using antibodies raised against a polypeptide derived from MAP65-4 (Smertenko *et al.*, 2008). Similar discrepancies also have been reported for MAP65-1 localization when different methods were applied (Smertenko *et al.*, 2008; Lucas & Shaw, 2012).

These seemingly conflicting results prompted us to investigate the function of MAP65-4 in cell division *in planta* in *A. thaliana*. Previously we demonstrated that MAP65-1 would largely acquire the function of MAP65-3 when it was artificially fused with the C-terminal domain of MAP65-3 and expressed under the control of the *MAP65-3* promoter (Ho *et al.*, 2012). Because MAP65-4, but not other MAP65 isoforms, contains an extended C-terminal sequence with significant homology to MAP65-3, these two most

closely related isoforms might bear similar functions in cytokinesis. Here we generated direct evidence supporting the hypothesis that in the absence of MAP65-3, remaining MT organization tasks during cytokinesis would be accomplished by a functionally redundant protein. Our results indicated that mutations at the *MAP65-3* and *MAP65-4* loci are synthetically lethal. Furthermore, MAP65-4 was detected at the phragmoplast midzone when it was expressed at a physiologically relevant level. MAP65-4 also marked the cortical cell division site after the disassembly of the PPB. Surprisingly, introduction of an extra copy of the *MAP65-4* gene in the *map65-3* mutant restored plant growth to a level very close to the wild-type control. Thus, these results revealed novel, cooperative functions of MAP65-3 and MAP65-4 in the organization of the phragmoplast MT array and cytokinesis.

Materials and Methods

Plant materials and growth conditions

Mutant seeds of *A. thaliana* (L.) Heynh. were obtained from the Arabidopsis Biological Research Center (ABRC) located at the Ohio State University in Columbus, Ohio, or obtained from Dr B. Favery at CNRS in France. These include the SALK_022166 and *dyc283* lines for the *MAP65-3*/At5g51600 locus as previously reported (Caillaud *et al.*, 2008; Sasabe *et al.*, 2011), and SALK_055682 for the *MAP65-4*/At3g60840 locus. The SALK lines are in the Columbia background and the *dyc283* mutant in the Ws background. All plants were grown in the growth chamber located on the University of California in Davis campus as described previously (Kong *et al.*, 2010).

Mutant lines were screened by standard PCR using the following primer sets: 22166LP (5′-TTTGAAATTCAAAAGTT CGAAAAAG-3′) and 22166RP (5′-GCAGTGTAACTCTTCA AGCTTTCTC-3′) for SALK_022166; 55682LP (5′-GATG AATGTATCCCTCTTATCATGC-3′) and 55682RP (5′-ATT CTTCACAACATCTTCTTCTTGG-3′) for SALK_055682; and the T-DNA-specific primer LBa1 (5′-TGGTTCACG TAGTGGGCCATCG-3′). The wild-type allele was detected by the combination of LP and RP primers, and the corresponding T-DNA insertions by LBa1 and RP primers.

Agrobacterium-mediated transformation experiments were carried out according to protocols described in our earlier report (Ho *et al.*, 2012). Transformants were selected on agar medium containing hygromycin before being planted in soil.

Recombinant DNA and expression vector construction

The genomic fragment of MAP65-4 including 1538 bp 5′ non-coding region was amplified using the primer pair 5′-CA CCGACGACGGCGACGATGAAGAGAG-3′ (forward) and 5′-GCAAAAACCGGCCCTAACCTCTTC-3′ (reverse) by using Phusion DNA polymerase (Thermo Fisher, Waltham, MA, USA). The PCR product was first cloned into the Gateway pENTR/D-TOPO vector (Invitrogen) to establish the pENTR-MAP65-4 plasmid. This plasmid was used as the donor for

recombination by the LR recombination reactions with the destination vectors pGWB4 (Nakagawa *et al.*, 2007), resulting in pGWB4-MAP65-4 aimed for expression of MAP65-4-GFP. The expression vectors of MAP65-3 were adopted from our previous study (Ho *et al.*, 2012).

Selection of the *map65-3*; *map65-4* lines complemented by MAP65-3 and MAP65-4

The MAP65-3-GFP expression vector (Ho *et al.*, 2012) and pGWB4-MAP65-4 plasmid, respectively, were transformed into the *map65-3* (−/−); *map65-4* (+/−) mutant plants. Among mutant plants expressing MAP65-3-GFP, the homozygous *map65-4* mutation was determined using the primers described in the section above. To isolate plants expressing MAP65-4 in the homozygous double mutation background, a new primer III60840veri (5′-GATACATGGTGTAGCAGCTTTC-3′) located in the 3′ untranslated region was used in combination with 55682RP (see later Supporting Information Fig. S3), which would detect the wild-type MAP65-4 locus by rendering a 3378 bp product but not the MAP65-4-GFP fusion.

Real-time reverse transcription (RT)-PCR experiments

Total RNA was isolated from 3-d-old etiolated seedlings with the Trizol Plus RNA Purication kit (Thermo Fisher). The cDNA samples were prepared using the iScript reverse transcription mix (Bio-Rad). The PCR primers for AtMAP65-4 were 5′-TCCAACTCTTTCAGGGAGGAGA-3′ and 5′-CTTTTCCTGCAACCGGAACG-3′. The primers for PP2a were synthesized as described by Czechowski *et al.* (2005). Triplicate real-time PCR amplifications were performed with 2 μl of each diluted cDNA in a 20 μl reaction containing the iTaq Universal SYBR Green Supermix (Bio-Rad) using the CFX96 Real-Time PCR Detection System (Bio-Rad). The relative quantification of transcripts was calculated based on a published method (Pfaffl, 2001). Assessment of the AtMAP65-4 expression levels was normalized to that of PP2a.

Fluorescence microscopy

Root meristematic cells were fixed and prepared from root squashes for indirect immunofluorescence staining as described previously (Lee & Liu, 2000). Primary antibodies used in this study included monoclonal mouse anti-GFP antibody (Covance, Princeton, NJ, USA), polyclonal goat anti-tubulin antibodies (Cytoskeleton, Denver, CO, USA) and polyclonal rabbit anti-MAP65-3 (Ho *et al.*, 2011). Secondary antibodies were fluorescein isothiocyanate (FITC)-conjugated donkey anti-mouse IgG, FITC-conjugated donkey anti-rabbit IgG and Texas Red-conjugated donkey anti-goat IgG (Rockland Immunochemicals, Gilbertsville, PA, USA). Stained cells were observed under an Eclipse 600 microscope equipped with 60× Plan-Apo and 100× Plan-Fluor objectives (Nikon) and images were acquired by an Orca CCD camera (Hamamatsu) using the METAMORPH software package (Molecular Devices).

Live-cell imaging was performed under an LSM710 laser scanning confocal module mounted on an Axio Observer inverted microscope using 40× C-Plan (water) or 63× Plan-Apo (oil) objectives (Zeiss). Images were acquired using the standard settings for enhanced GFP using the ZEN software package, and processed in IMAGEJ (www.imagej.nih.gov/ij). All micrographs were assembled into plates in Adobe PHOTOSHOP (Adobe).

Accession numbers

The Arabidopsis Information Resource locus identifier for the genes mentioned in this article are At5g55230 for MAP65-1, At5g51600 for MAP65-3 and At3g60840 for MAP65-4.

Results

MAP65-4 is closely related to MAP65-3 and their simultaneous losses lead to lethality

The MAP65 family proteins exhibit high degrees of sequence divergence toward their C-termini (Smertenko *et al.*, 2008). Among nine MAP65 isoforms in *A. thaliana*, MAP65-3 and MAP65-4 are the largest having 707 and 677 amino acids, respectively, while other isoforms are peptides of 550–600 amino acid (Fig. S1). Compared with MAP65-1, MAP65-4 also demonstrates higher sequence homology to MAP65-3 (Fig. 1a). Only MAP65-3 and MAP65-4 have the C-terminal extensions over 100 amino acids that share sequence identity/similarity of 31.7%/45.3%, while others have extensions shorter than 50 amino acids that have little if any homology to MAP65-3 or MAP65-4. Because the *MAP65-3* and *MAP65-4* genes exhibit similar cell cycle-dependent expression patterns although MAP65-4 has a significantly lower overall expression level than MAP65-3 (http://jsp.weigelworld.org/expviz/expviz.jsp), we postulated that MAP65-4 shared similar functions with MAP65-3 while the latter was more dominant.

We then tested the function of MAP65-4 by isolating a homozygous mutant in which a T-DNA fragment was inserted in the second exon (Fig. 1b). The homozygous mutant grew similarly to the wild-type control under tested conditions in the growth chamber (Fig. 1c,d). Therefore, we attempted to generate double mutants of *map65-3* and *map65-4* and successfully isolated the *map65-3/map65-3*; *MAP65-4/map65-4* mutant but not double homozygous mutants after analyzing three generations of segregants resulting from self-crosses. Compared with the *map65-3* single mutant, this *map65-3/map65-3*; *MAP65-4/map65-4* mutant exhibited a consistent phenotype of enhanced overall growth retardation (Fig. 1c,d). However the *map65-3/map65-3*; *MAP65-4/map65-4* mutant was still be able to undergo vegetative growth and sexual reproduction.

Previously, it was demonstrated that null *map65-1* or *map65-2* mutations enhanced the growth phenotypes brought about by *map65-3* (Sasabe *et al.*, 2011). We compared the growth phenotypes of the *map65-3/map65-3*; *MAP65-4/map65-4* mutant with *map65-3/map65-3*; *map65-1/map65-1*, and found that the *map65-3/map65-3*; *MAP65-4/map65-4* mutant consistently
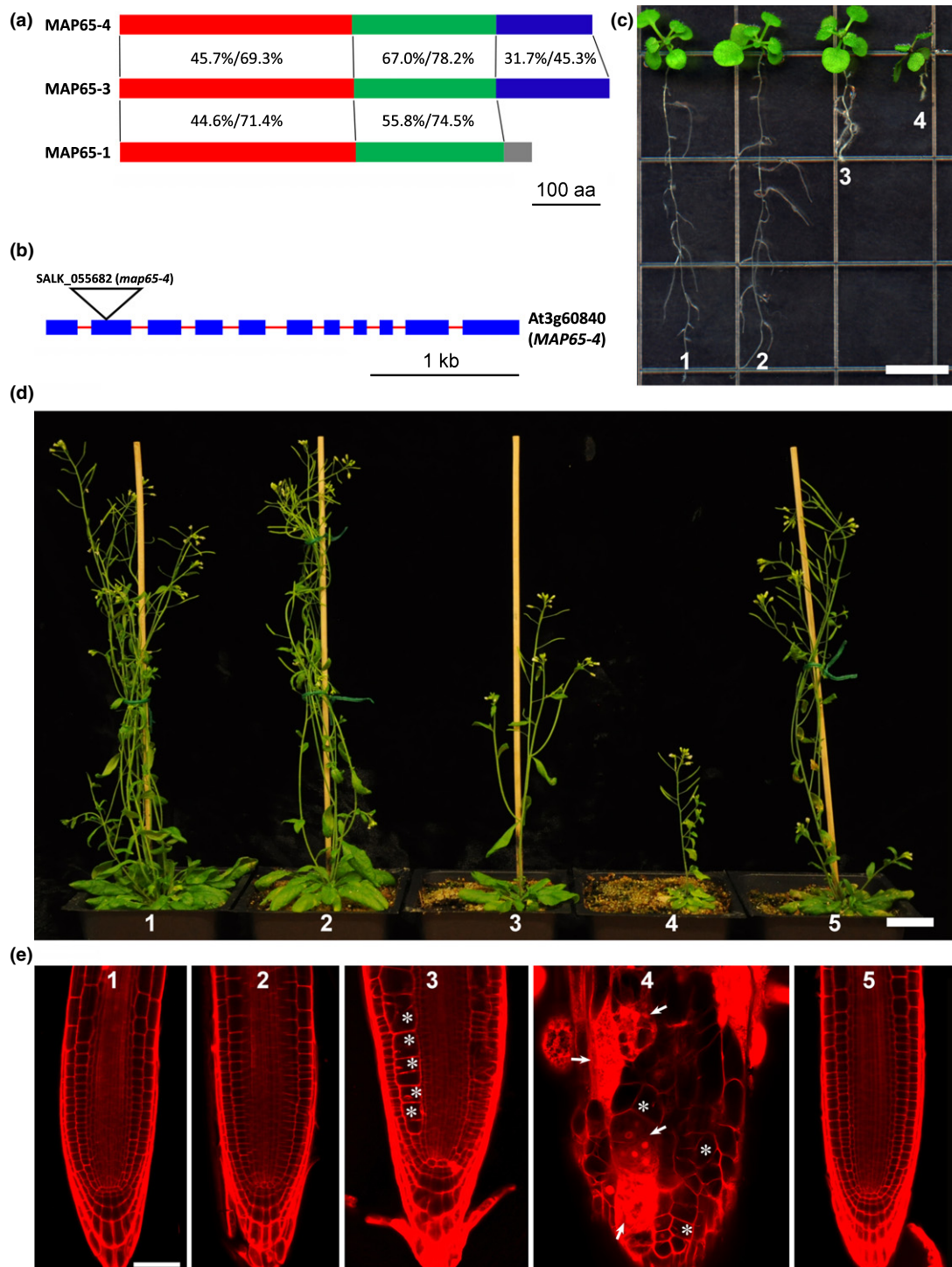
Fig. 1 Synergistic functions of MAP65-3 and MAP65-4 in cytokinesis and seedling growth in *Arabidopsis thaliana*. (a) Overall sequence homologies among MAP65-3, MAP65-4 and MAP65-1. The polypeptides are divided into three regions: the N-terminal dimerization domain (red), the central microtubule (MT)-binding domain (green) and the C-terminal variable domain (blue and gray). The numbers reflect amino acid sequence identities/similarities; aa, amino acids. (b) Schematic diagram illustrating the gene structure with exons in blue boxes and introns in red lines. The T-DNA insertional site is indicated. (c) Comparison of 10-d-old seedlings of the wild-type control (1), *map65-4* (−/−) (2), *map65-3* (−/−) (3) and *map65-3* (−/−); *map65-4* (+/−) (4) mutants. (d) Comparison of mature plants of the wild-type control (1), *map65-4* (−/−) (2), *map65-3* (−/−) (3), *map65-3* (−/−); *map65-4* (+/−) (4), and *map65-3* (−/−); *map65-4* (−/−) mutant expressing MAP65-3 (5). (e) The *map65-3* and *map65-4* mutations cause cytokinetic defects in root cells as demonstrated by PI staining. While cell division takes place normally in both the wild-type control (1) and *map65-4* (−/−) (2) mutant, frequently cell wall stubs are found in the *map65-3* (−/−) cells that are the result of incomplete cytokinesis (asterisks, 3). The *map65-3* (−/−); *map65-4* (+/−) plant exhibits aggravated cytokinetic defects by forming gigantic dead cells with strong autofluorescence (arrows, 4) while others had cell wall stubs (asterisks, 4). Genetically suppressed *map65-3* (−/−); *map65-4* (−/−) mutant by *MAP65-3* allows the formation of roots similar to the wild-type control (5). Bars: (c) 1 cm; (d) 5 cm; (e) 50 μm.

showed a much more retarded growth phenotype when compared with the latter (Fig. S2). This surprising finding suggested that the amount of MAP65-4 protein became critical and it became indispensable in the absence of MAP65-3.

We performed genetic suppression or complementation experiments aimed at rescuing the *map65-3*/ *map65-3*; *map65-4*/ *map65-4* double homozygous mutant by expressing MAP65-3-GFP under the control of its native promoter in the host of heterozygous *map65-3*/ *map65-3*; *map65-4*/ *map65-4* plants. Indeed, homozygous *map65-3*/ *map65-3*; *map65-4*/ *map65-4* mutants were rescued upon expressing MAP65-3 (Fig. 1d).

Unlike the *map65-3* null mutation which caused serious defects in cytokinesis as revealed in roots when cells were outlined by propidium iodide (PI) staining, the *map65-4* homozygous mutant did not show a noticeable defect in this aspect and its root resembled that of the wild-type control (Fig. 1e). The loss of a single *MAP65-4* copy in the *map65-3* homozygous mutant, however, led to greatly enhanced defects in root cell division, as shown by the appearance of cells with multiple nuclei stained by PI, which had a consequence of deforming and swelling roots (Fig. 1e). This phenotype was suppressed when *MAP65-3* was introduced by transformation, as demonstrated in the background of the *map65-3*; *map65-4* double homozygous mutation (Fig. 1e). Hence, we interpreted that the enhanced growth defects

upon introduction of the *map65-4* mutation was concomitant with the aggravation of cytokinesis defects in the *map65-3* mutant.

We then investigated the cause of the inability to produce a homozygous double mutant. We first examined the siliques produced by the *map65-3*/ *map65-3*; *MAP65-4*/ *map65-4* mutant. There were many white unfertilized ovules or aborted seeds juxtaposed to developing seeds that resulted from successful fertilization, while both wild-type control and either *map65-3* or *map65-4* mutant produced siliques filled with seeds (Fig. 2a). To determine how sexual reproduction was affected, we performed reciprocal pollinations between the *map65-3*/ *map65-3*; *MAP65-4*/ *map65-4* mutant and the wild-type control. Analysis of the genotypes of the progeny derived from the crosses indicated that the transmission efficiency was 23.7% through the male gametophyte and 0.08% through the female gametophyte (Table 1). Therefore, both the male and the female gametophytes experienced great difficulties in inheriting the *map65-3* and *map65-4* mutations together, suggesting that the gametogenesis depended on the collective function of MAP65-3 and MAP65-4. We thus examined developing gametophytes produced by the *map65-3*/ *map65-3*; *MAP65-4*/ *map65-4* mutant. When the ovules were cleared for observation, defective ovules were found to have contained either one or two nuclei while the wild-type control ovules
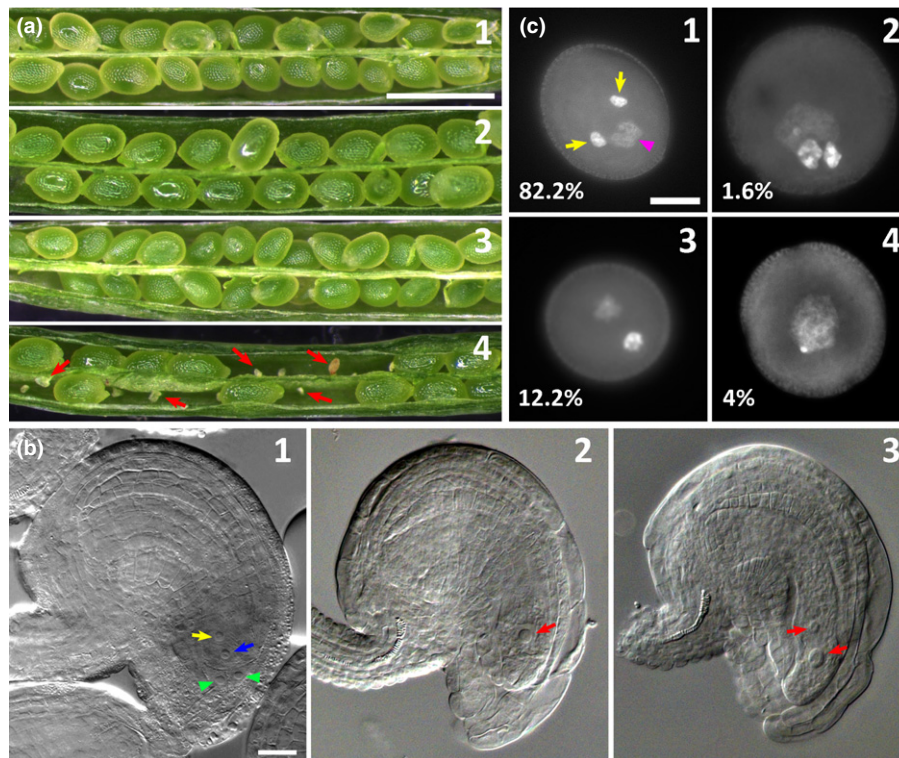

Fig. 2 The *map65-3* and *map65-4* double mutant is gametophytically lethal in *Arabidopsis thaliana*. (a) Siliques of the wild-type control (1), *map65-3* (−/−) (2) and *map65-4* (−/−) (3) are filled with developing seeds but that of *map65-3* (−/−); *map65-4* (+/−) (4) contains many small unfertilized ovules (red arrows). (b) Compared with the wild-type ovule that contains an egg (blue arrow), a central nucleus (yellow arrow) and two synergids (green arrowheads, 1), mutant ovules often contain a single or two nuclei (red arrows, 2 and 3) that are suspended in the same cytoplasm. (c) Defects of male gametophyte/pollen. The heterozygous *map65-3* (−/−); *map65-4* (+/−) parent plant produced normal pollen grains (1) with two sperms with dense chromatin (yellow arrows) and a vegetative nucleus (magenta arrowhead), resembling those produced by the wild-type control, and defective pollen grains containing either three nuclei (2), two nuclei (3) or a single nucleus (4). The percentages of each pollen type is indicated on the micrographs (*n* = 428). Bars: (a) 1 mm; (b) 20 μm; (c) 10 μm.

Table 1 Reciprocal crosses between the wild-type (WT) and the *map65-3* (−/−); *map65-4* (+/−) plants and transmission efficiency (TE) of the *map65-4* mutation in *Arabidopsis thaliana*

| ♀ Parent | ♂ Parent | Progeny genotype at the MAP65-4 locus | | map65-4 TE |
		+/−	+/+	
WT	*map65-3* (−/−); *map65-4* (+/−)	32	135	♂ gamete TE = 23.7%
map65-3 (−/−); *map65-4* (+/−)	WT	2	251	♀ gamete TE = 0.8%

TE is calculated as the number of (+/−) progeny over those of (+/+) as a percentage.

clearly produced an egg cell and two synergids (Fig. 2b). The suspension of irregular numbered and shaped nuclei indicated defects in the cellularization process. Furthermore, we examined pollen grains produced by the mutant and found frequently aborted male gametogenesis. In addition to *c.* 6% pollen grains that were shrunken, fully enlarged pollen grains often contained a single nucleus or two nuclei while the wild-type pollen grains always showed two sperm nuclei and one vegetative nucleus (Fig. 2c). In other instances, pollen grains were often enlarged while remaining with a tricellular appearance. The heterozygous mutant produced over 17% defective pollen grains (Fig. 2c) that were seen perhaps once in a thousand times among those produced by the wild-type plant.

Collectively, these results indicated that the enhanced growth defects in the *map65-3/ map65-3*; *MAP65-4/ map65-4* mutant when compared with the *map65-3/ map65-3* single mutant were indeed caused by the reduced gene dose of *MAP65-4* and that the *map65-4* mutation was synthetically lethal with *map65-3*. The synthetic lethality was caused by loss of the overlapping functions of MAP65-3 and MAP65-4 in cross-linking antiparallel MTs in the phragmoplast and consequently cytokinesis failures during both gametophyte and embryo development.

MAP65-4 localizes to the PPB, mitotic spindle and phragmoplast

To examine the intracellular localization of MAP65-4, a GFP fusion protein was expressed under the control of its native promoter in the *map65-4* homozygous mutation background. The

anticipated functionality of this fusion protein was first based on the fact that a similar C-terminally GFP-tagged MAP65-3 fusion protein was determined to be fully functional (Ho *et al.*, 2012). This was further confirmed by suppression of the *map65-3/ map65-3*; *map65-4/ map65-4* double homozygous mutant (Fig. S3). The MAP65-4-GFP signal was first discerned in the PPB, as thin filaments or dense bundles (Fig. 3a,b). As cell division progressed into mitosis, MAP65-4 localized to spindle structures with signals emphasized toward the middle region (arrows, Fig. 3c,d). The signal became conspicuous around the division site and culminated in the phragmoplast with bright signals in the midzone (Fig. 3e,f).

Furthermore, dual localization experiments were also carried out to show the relationship between MAP65-4 and MTs (Fig. 4). As revealed by immunofluorescence microscopy with anti-GFP and anti-tubulin antibodies, MAP65-4 decorated the PPB and colocalized with the PPB MTs (Fig. 4a). However, MAP65-4 was not detected on the nuclear envelope where abundant perinuclear MTs were apparent (Fig. 4a). At metaphase, MAP65-4 was particularly pronounced the middle region of the spindle, decorating MT bundles crossing the metaphase plate while being barely detectable elsewhere in the spindle (Fig. 4b). In addition, MAP65-4 remained at the cortical site previously occupied by the PPB after the disassembly of the PPB MTs (arrowheads, Fig. 4b). Upon completion of chromosome segregation, MAP65-4 was associated with MT bundles in the central spindle, and in particular decorating the middle zone of the MT array (arrows, Fig. 4c). When the bipolar phragmoplast MT array became conspicuous, MAP65-4 became intensely concentrated
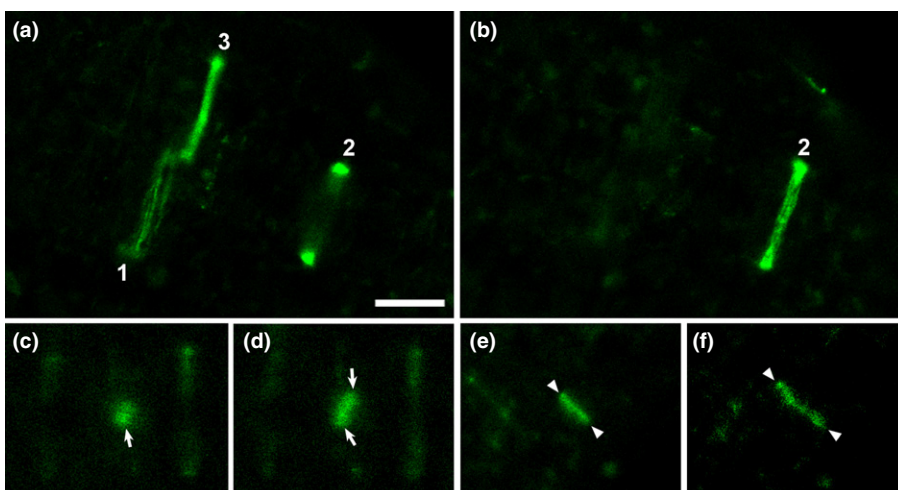
Fig. 3 MAP65-4-GFP localization in living root cells in *Arabidopsis thaliana*. (a,b) MAP65-4 decorates preprophase band-like structures from a fine broad localization pattern (1) to narrow and tight ones (2, 3) in two different focal planes. (c,d) MAP65-4-GFP marks the midzone of mitotic spindles at two different stages (arrows). (e,f) The phragmoplast is marked by the MAP65-4 fusion protein with signals more conspicuous toward the midline (arrowheads). Bar, 10 μm.
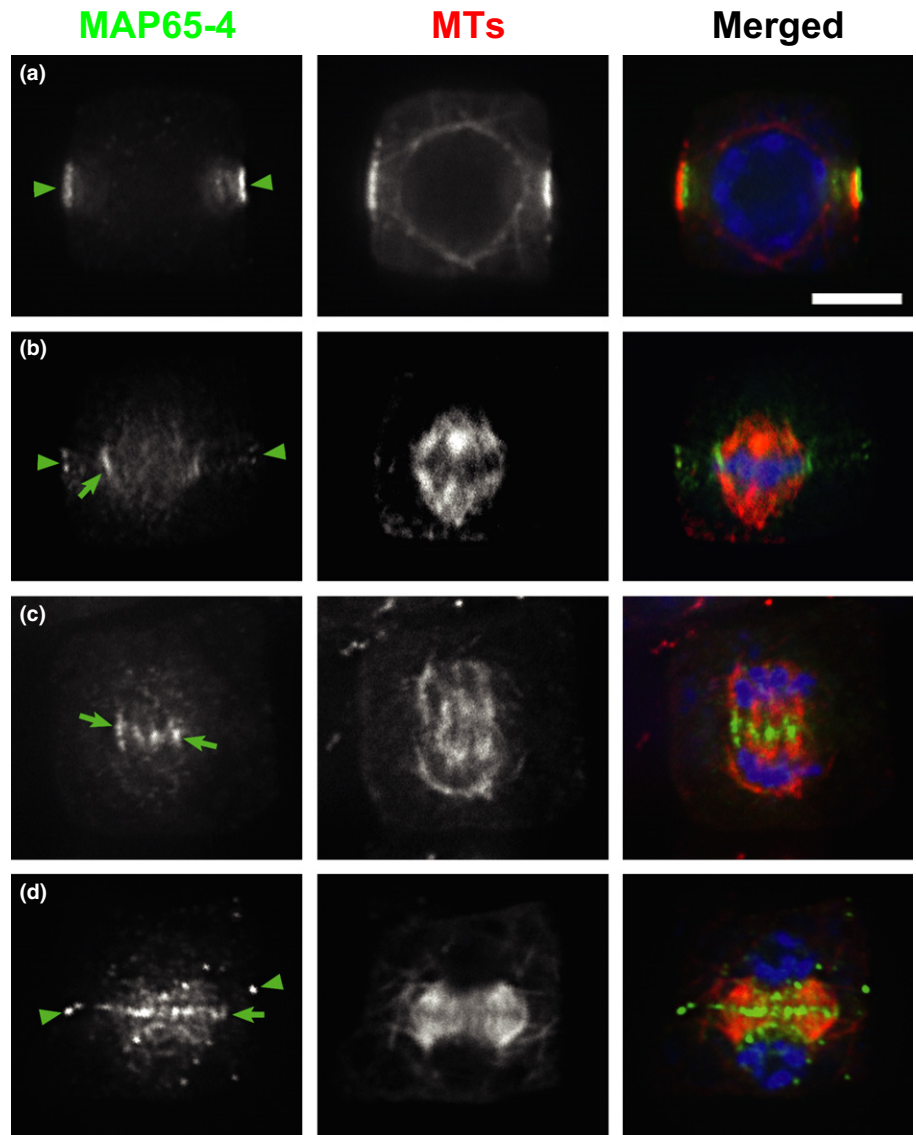
MAP65-4 **MTs** **Merged**

Fig. 4 Localization of MAP65-4-GFP with microtubules (MTs) as the reference in root meristematic cells in *Arabidopsis thaliana*. The merged images have MAP65-4-GFP detected by the anti-GFP antibody in green, MTs in red and DNA in blue. (a) MAP65-4 exclusively labels the preprophase band (arrowheads), but not the perinuclear MTs. (b) MAP65-4 is detected in the middle region of the metaphase spindle (arrow) and the cortical division site (arrowheads). (c) At late anaphase/telophase, MT bundles in the middle region of the developing central spindle are markedly labeled by MAP65-4 (arrows). (d) MAP65-4 can be detected in the phragmoplast midline (arrow) and elsewhere on MTs such as the distal ends while its signal still is found at the cortical division site (arrowheads). Bar, 5 μm.

in a narrow region where anti-parallel phragmoplast MTs interdigitated while being present elsewhere in the phragmoplast such as the distal ends facing the daughter nuclei (arrow, Fig. 4d). In addition to the localization on phragmoplast MTs, the protein was again detected at the cortical division site as concentrated dots (arrowheads, Fig. 4d). This pattern suggested that MAP65-4 perhaps underwent some kind of reorganization while persisting at the cortical division site occupied by the PPB.

Comparison of MAP65-4 and MAP65-3 localizations

The localization of MAP65-4 in the midzone of anaphase central spindle and the midzone of the phragmoplast prompted us to compare it to that of MAP65-3, which is particularly concentrated in those regions. To do so, MAP65-4 and MAP65-3 were detected simultaneously by immunolocalization experiments using an anti-GFP antibody to detect MAP65-4-GFP and monospecific anti-MAP65-3 antibodies in the *map65-4* null mutant cells expressing MAP65-4-GFP (Ho *et al.*, 2011).

Differences in their localizations were discerned in three aspects (Fig. 5). First, although both proteins were detected in the PPB, MAP65-4 was significantly more conspicuous when the cytoplasmic diffuse signal was used as a reference (arrowheads, Fig. 5a). While MAP65-3 disappeared upon the disassembly of PPB MTs, MAP65-4 remained at the cortical division site (arrowheads, Fig. 5b). Second, MAP65-4 was associated with MTs in the central region of the metaphase spindle where MAP65-3 was never detected (arrows, Fig. 5b). This suggests that the localization of MAP65-3 and MAP65-4 in mitotic cells is differentially regulated even though they both are preferentially expressed in dividing cells. Lastly, the gradual accumulation and dynamics of MAP65-4 in the developing phragmoplast were different from the exclusive localization of MAP65-3 in the phragmoplast midline, highlighting the overlapping region of the anti-parallel MTs (Fig. 5b). MAP65-4 not only decorated the middle zone of the phragmoplast, but was also detected elsewhere in the phragmoplast, in particular toward the distal ends (Fig. 5b). The difference in their phragmoplast localizations further stressed the
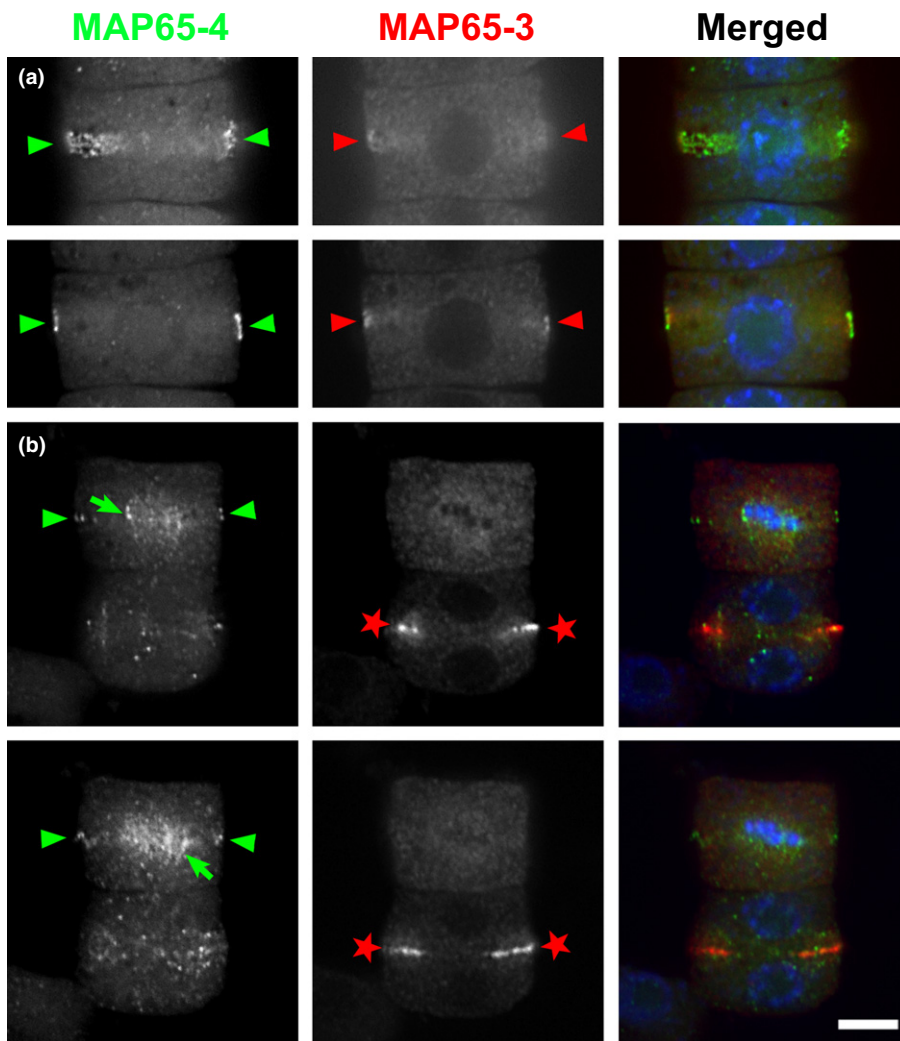
MAP65-4 **MAP65-3** **Merged**

Fig. 5 Comparison of MAP65-3 and MAP65-4 localizations in root cells in *Arabidopsis thaliana*. The merged images have MAP65-4-GFP detected by the anti-GFP antibody in green, MAP65-3 in red and DNA in blue. (a) MAP65-4 conspicuously decorates in the preprophase band where MAP65-3 is also detected (arrowheads). Two optical sections are shown here. (b) MAP65-4 is detected in the metaphase spindle, marking the microtubule (MT) bundles that trespass the metaphase plate (arrows). However, MAP65-3 is absent from the spindle. In addition, MAP65-4, but not MAP65-3, remains at the cortical division site at metaphase (arrowheads). In the phragmoplast, MAP65-3 exclusively decorates the midline (stars). However, MAP65-4 shows more discrete localization with signals in the midline as well as distal ends, and scarcely elsewhere on MTs. Two optical sections are shown. Bar, 5 μm.

hypothesis that the two MAP65 isoforms are targeted to sites on mitotic MT arrays through mechanisms beyond their bundling activities in dividing cells.

Introduction of an extra copy of MAP65-4 suppresses the *map65-3* mutation

MAP65-3 plays a critical role in engaging the anti-parallel MTs in the phragmoplast and other important factors for cytokinesis such as Kinesin-12 depend on MAP65-3 for their localization in the phragmoplast midzone (Ho *et al.*, 2011). Therefore, we tested whether the localization of MAP65-4 was dependent on MAP65-3. To do so, the MAP65-4-GFP fusion was expressed under the control of its native promoter in the *dyc283* mutant, which lacked the MAP65-3 protein, as we have reported (Ho *et al.*, 2011). When transgenic plants were examined, to our surprise they consistently exhibited much improved growth in terms of primary root length, leaf dimensions, plant height and reproduction when compared with the *dyc283* mutant (Fig. 6). We found that the cytokinesis defects in the *map65-3* mutant cells were greatly suppressed by the introduction of an extra copy of MAP65-4 (Fig. S4). We hypothesized that the growth defects

brought about by the *map65* null mutation were suppressed by elevated expression of MAP65-4. To test this, we performed real-time RT-PCR experiments. Compared with the wild-type seedlings, the *map65-3* mutant had a very similar expression level of MAP65-4, 0.99 ± 0.16 vs 0.98 ± 0.16, while it was undetectable in the *map65-4* mutant (Fig. S5). By contrast, it was elevated to 3.92 ± 1.19 in the transgenic *map65-3* line ectopically expressing MAP65-4-GFP (Fig. S5). Therefore, this result supported our hypothesis. It also suggested that without the dominant function of MAP65-3 in the phragmoplast, cell division became sensitive to the dosage of MAP65-4. It further supported the notion that MAP65-4 functioned in cytokinesis.

Therefore, we further examined the function of MAP65-4 in cytokinesis by examining MT organization during cytokinesis in the *map65-3* mutant alone and that expressing MAP65-4. In wild-type cells at late stages of anaphase, MTs in the central spindle were arranged in continuous parallel bundles between segregated chromosomes (arrows, Fig. 7a). In the control cells undergoing cytokinesis, MTs from the two half-phragmoplasts often formed mirrored bundles that left a very narrow 'gap' in the middle when revealed by anti-tubulin immunofluorescence (arrowheads, Fig. 7b, c). This phenomenon again reflected the engagement of anti-

Fig. 6 Suppression of the *map65-3* mutation by elevated expression of MAP65-4 in *Arabidopsis thaliana*. (a) Seven-, (b) 40- and (c) 60-d-old seedlings/plants of the *dyc283/map65-3* mutant (1), *dyc283* with MAP65-4 (2), and the wild-type (Ws ecotype) control (3). The addition of an extra copy of MAP65-4 enhances (a) root growth, (b) leaf expansion, and (c) overall vegetative and reproductive growth. Bars: (a) 1 cm; (b,c) 2 cm.

parallel MTs in the phragmoplast as we have demonstrated in the past (Ho *et al.*, 2011). The loss of MAP65-3 in the *map65-3* null mutant led to obvious disengagement of MTs emanating from sister chromatids so that a large zone devoid of MTs was seen in the central spindle (asterisks, Fig. 7d). The *map65-3* phragmoplast is characterized to have a wide gap in the middle (asterisks, Fig. 7e,f), recapitulating what has been previously reported (Müller *et al.*, 2004; Ho *et al.*, 2011). Due to the disengagement of anti-parallel MTs derived from the two half-phragmoplasts, the MTs often flared outwards, instead of assuming 90° to the division plane (arrows, Fig. 7f). The introduction of ectopic MAP65-4 in the *map65-3* mutant not only restored the parallel MT bundles in the anaphase central spindle (arrows, Fig. 7g), but also narrowed the middle gap in the phragmoplast (Fig. 7h,i). Therefore, we concluded that suppression of the *map65-3* mutation was due to the re-engagement of anti-parallel MTs in the phragmoplast brought about by the incremental supplement of MAP65-4.

Localization of ectopically supplied MAP65-4 in the *map65-3* mutant cells

Because the introduction of this extra copy of MAP65-4 seriously suppressed the cytokinesis defects in the *map65-3* mutant, we examined the localization of this MAP65-4-GFP fusion protein by immunofluorescence. MAP65-4-GFP localization to the PPB and the middle region of metaphase spindles was similar to what was seen in cells expressing MAP65-3 (Fig. 8a,b). Toward the end of anaphase and at telophase, MAP65-4 became concentrated in the middle region of central spindle MTs while continuously being present at the cortical division site as discontinuous particles, sometimes in punctate patterns (Fig. 8c). Its localization in developing phragmoplasts was particularly conspicuous (Fig. 8d,e). Compared with its localization in cells expressing MAP65-3, the signal became highly concentrated in the midzone in a very restricted space (arrows, Fig. 8d,e). This notion was further supported by a close comparison of MAP65-4 localization in the presence or absence of MAP65-3 (Fig. 9). In cells expressing the wild-type MAP65-3, MAP65-4 was not only conspicuously enriched in the phragmoplast midline but also detected toward the distal (minus) ends of phragmoplast MTs, as clearly illustrated by a fluorescence intensity scan (Fig. 9a). In the *map65-3* mutation background, however, MAP65-4 became totally concentrated in the phragmoplast midline (Fig. 9b). This finding strengthened the notion that MAP65-4, when expressed at elevated levels, perhaps assumed the function normally exercised by MAP65-3 to bundle anti-parallel MTs in the phragmoplast. The result further explained that because of introducing an extra copy of the *MAP65-4* gene in the absence of MAP65-3, anti-parallel phragmoplast MTs became engaged again due to the substitution of MAP65-3 function by MAP65-4. Consequently, cytokinesis became more successful than the control *map65-3* mutant that would lead to improved growth and reproduction.

We then investigated whether the loss of MAP65-4 would alter the localization of MAP65-3. To do so, MAP65-3 was detected in the *map65-4* mutant cells by immunolocalization (Fig. S6). MAP65-3 was weakly detected on the PPB (arrowheads, Fig. S6a).
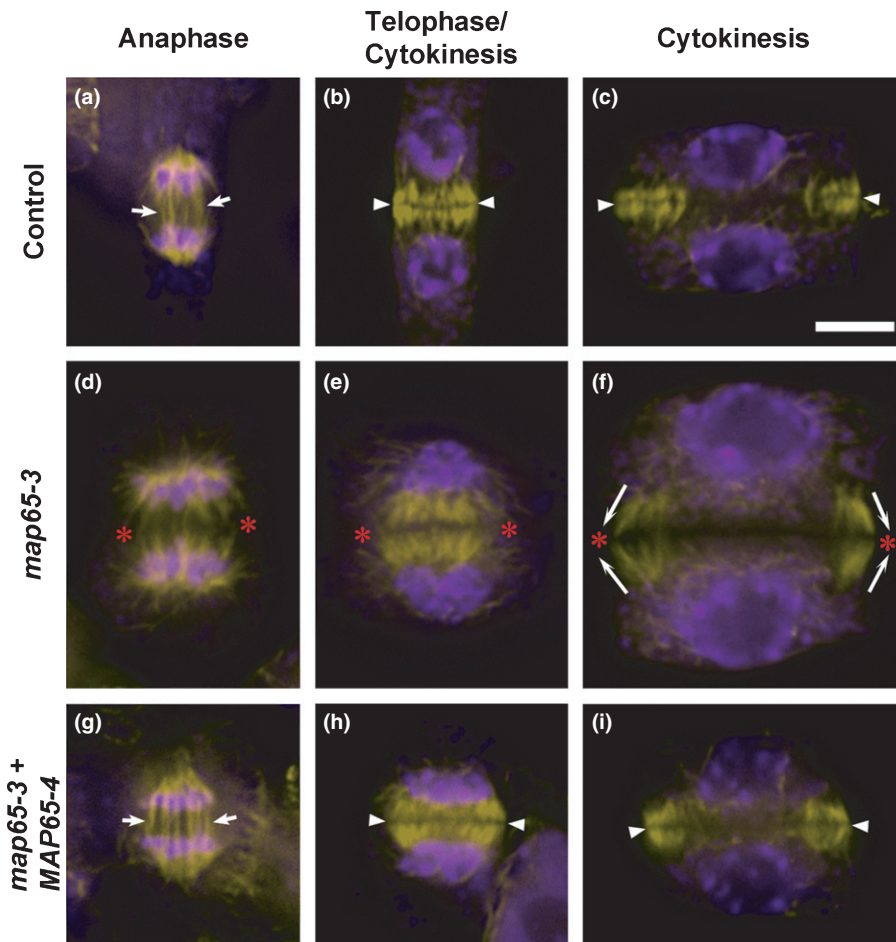
Fig. 7 Re-engagement of anti-parallel microtubules (MTs) in developing phragmoplasts in the *map65-3* cells by MAP65-4 in *Arabidopsis thaliana*. MTs are pseudocolored in yellow and DNA in magenta. (a–c) Wild-type cells at anaphase, telophase and cytokinesis. (d–f) The *dyc283/map65-3* cells at similar stages as the wild-type control. (g–i) The *dyc283/map65-3* cells expressing additional MAP65-4 in the GFP fusion. At anaphase, the control cell shows parallel MT bundles running between segregated chromatids (arrows, a). The *dyc283/map65-3* cell at anaphase shows loose, disengaged MT bundles emanating from segregated chromatids that leave a wide unoccupied zone in the middle (asterisks, d). This mutant phenotype was corrected when cells express extra MAP65-4 (arrows, g). In the phragmoplast, MT bundles are well engaged from two half-phragmoplasts, leaving a very narrow dark line under fluorescence microscopy (arrowheads, b,c). In the *dyc283/map65-3* mutant cells at similar stages, MTs display loose bundles and leave a wide gap in the middle, indicating that they are not well engaged. Because of the disengagement, anti-parallel MTs often point outward toward the expanding edge of the phragmoplast, instead of being perpendicular to the division site (arrows, f). The MT organization defects in developing phragmoplasts of *dyc283/map65-3* mutant were largely corrected once extra MAP65-4 is produced, as indicated by narrowed midlines (arrowheads). Bar, 5 μm.

Only diffuse MAP65-3 signal was detected in the cytosol in cells possessing metaphase spindles (Fig. S6b). In telophase cells, the protein became concentrated in the midzone of the developing phragmoplast (arrows, Fig. S6c). Unlike MAP65-4, MAP65-3 was not detected at the cortical cell division site after disappearance of the PPB. Therefore, we concluded that MAP65-3 behaved similarly in the *map65-4* mutant and the wild-type control cells. Furthermore, our data indicated that the activities of MAP65-4 in the metaphase spindle midzone and cortical division site after PPB disassembly were irreplaceable by MAP65-3.

Discussion

MAP65 family proteins are often known for their evolutionarily conserved function in cytokinesis by regulating the organization of anti-parallel MT arrays in the spindle midzone as well as the plant phragmoplast and the animal midbody. The existence of multiple MAP65 isoforms in *A. thaliana* and other plants had raised the question of whether they all contribute to cytokinesis in a similar manner (Hamada, 2014). Our results revealed a novel phenomenon on the overlapping but unequal functions of two of the nine MAP65 isoforms in the phragmoplast in this model plant. While MAP65-3 plays a dominant role in phragmoplast MT organization and its loss leads to severe cytokinesis defects, we found that MAP65-4 also contributed such a function, although to a lesser extent. Perhaps this is why *A. thaliana* plants can survive in the absence of either isoforms but became completely inviable when both are lost. Our work also revealed a novel aspect on the differential contribution of the two isoforms as demonstrated by rescue of the *map65-3* null mutant by the introduction of an extra copy of the *MAP65-4* gene. Our findings suggest that these two isoforms are designated to function in MT organization in dividing cells while others
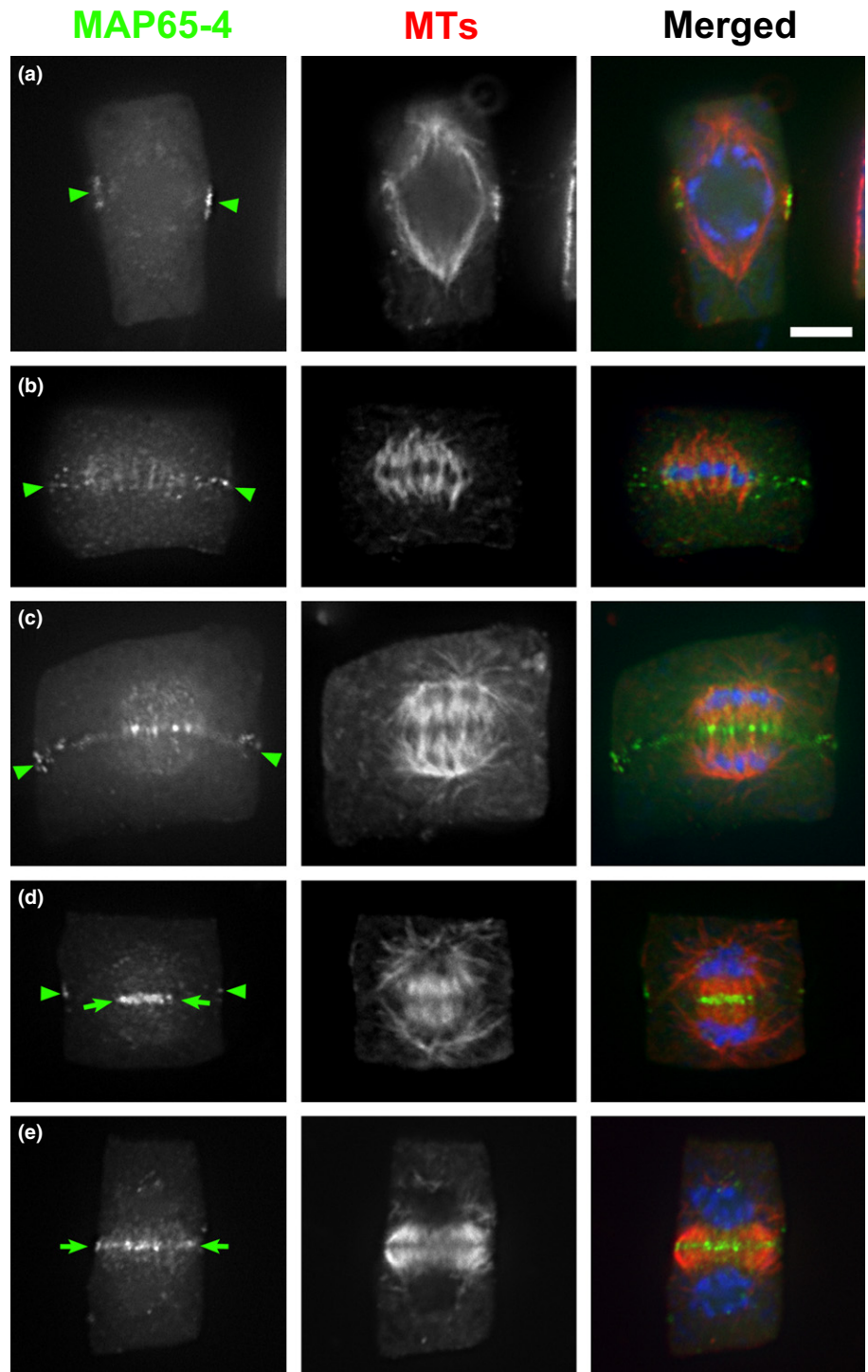
Fig. 8 Localization of MAP65-4 in the absence of MAP65-3 in root meristematic cells in *Arabidopsis thaliana*. The merged images have MAP65-4-GFP in green, microtubules (MTs) in red and DNA in blue. (a) MAP65-4 decorates the preprophase band but not the prespindle in a late prophase cell. (b) At metaphase, MAP65-4 labels the MT bundles in the midzone of the spindle and also exhibits discontinuous localization at discrete spots at the cortical division site (arrowheads). (c) At late anaphase or telophase, while continuously being present at the cortical division site (arrowheads), MAP65-4 becomes conspicuous in the midzone of the central spindle decorating the interface of apparent anti-parallel MTs. (d) In an early phragmoplast, MAP65-4 becomes highly concentrated in the midzone (arrows), bordering two sets of anti-parallel MTs. Remnant MAP65-4 signal was detected at the cortical division site (arrowheads) (e). In a mature phragmoplast, MAP65-4 becomes highly concentrated in the midline (arrows) while being less visible elsewhere on MTs. Bar, 5 μm.

perhaps function primarily at other stages of the cell cycle or in cells undergoing differentiation.

Isoform-specific expression pattern and localization of MAP65 family proteins

Our findings serve another line of evidence suggesting that the localization of MAP65 isoforms is spatially and temporally regulated. The results presented here and those from previous publications clearly indicate that MAP65-3 and MAP65-4 are mitotic isoforms that decorate mitotic MT arrays but not cortical MTs in interphase (Müller *et al.*, 2004; Caillaud *et al.*, 2008; Ho *et al.*, 2011). This localization pattern is consistent with the gene expression analysis that was based in community-generated microarray data as mentioned earlier. Conversely, MAP65-1 and MAP65-2 have a cell cycle-independent expression pattern because all cells have these proteins and decorate various MT arrays in plants expressing them under the control of their native
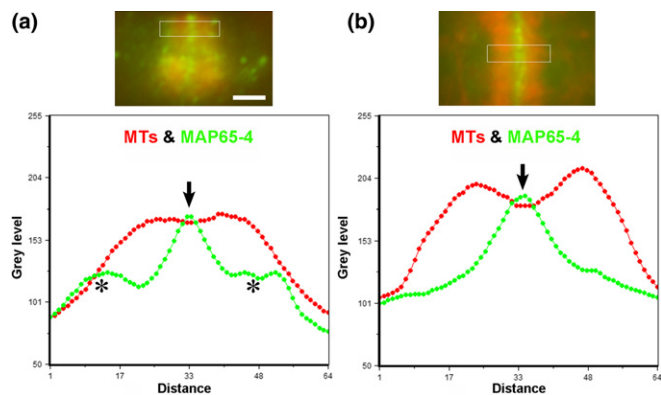
Fig. 9 Comparison of phragmoplast localization of MAP65-4 in the presence and absence of MAP65-3 in *Arabidopsis thaliana*. In the composite images shown at the top, microtubules (MTs) are pseudocolored in red and MAP65-4 in green. Quantitative assessments of the fluorescence intensities of MTs and MAP65-4 in the boxed regions are shown below the images, in which the distance is expressed in arbitrary units. (a) In the presence of MAP65-3, MAP65-4 exhibits localization toward the distal ends of phragmoplast MTs (asterisks) in addition to prominent decoration of the midzone (arrow). (b) In the *map65-3* mutation background, MAP65-4 is more or less restricted in the phragmoplast midzone (arrow), as illustrated by the fluorescence intensity scan. Bar, 2 µm .

promoters (Lucas & Shaw, 2012). Therefore, we suggest that MAP65-1/2 probably play general roles in supporting the overall stability and/or dynamics of the MT network in all cells.

Besides exhibiting different expression patterns, the MAP65 isoforms examined to date show drastically different intracellular localization patterns on MT arrays. Related data have been acquired by means of immunostaining of native proteins in meristematic or cultured cells, over expression of GFP fusion proteins in established cultured cells such as tobacco BY-2, and expression of GFP fusions under the native promoters within the system. Intuitively speaking, MAP65 proteins function as MT cross-linkers so that they should be evenly bundle MTs whenever and wherever they are present. Besides the distinct localization patterns of MAP65-3 and MAP65-4 shown here and previously, others showed unexpected localizations as well. For example, MAP65-6 exhibited a punctate localization pattern, and sometimes overlapping with mitochondria (Mao *et al.*, 2005; Smertenko *et al.*, 2008). Clearly, the localization of MAP65 isoforms is regulated. Two potential mechanisms may account for different localizations. First, they may be targeted to different regions of MTs via their interacting partners. For example, isoforms such as MAP65-3 may be concentrated toward the MT plus end via the plus end tracking protein EB1. However, it would not explain why certain isoforms selectively recognize a subpopulation of MTs in cells, for example PPB vs perinuclear MTs. Different C-terminal sequences may imply their interactions with different proteins, perhaps targeting factors. This is supported by our earlier finding that a chimeric MAP65-1 bearing the C-terminus of MAP65-3 assumed the localization pattern of the native MAP65-3 (Ho *et al.*, 2012). Alternatively, the localization may be post-translationally regulated, for example via phosphorylation. This is exemplified by the MAP65-1

counterpart(s) in tobacco cells in which phosphorylated forms selectively decorated the phragmoplast midzone while the unphosphorylated form decorated entire phragmoplast MTs (Sasabe *et al.*, 2006). Indeed, MAP65 family proteins from plants and of other origins are heavily phosphorylated, especially during the cell division cycle that directly influences their interaction with MTs (Smertenko *et al.*, 2006).

Sometimes different approaches resulted in inconsistent or even contradictory results regarding the localization of a particular MAP65 isoform. For example, MAP65-1 was detected in the phragmoplast toward the midzone in tissue cultured cells, although in a much wider range than MAP65-3 (Smertenko *et al.*, 2008). However, GFP fusions expressed under the control of its native promoter showed a nonselective decoration on all MTs in *A. thaliana* cells (Lucas & Shaw, 2012). The difference perhaps arose from the uses of different cell types or detection methods. By contrast, MAP65-3 has been consistently detected in the phragmoplast midline no matter what method was applied or what was the origin of the cells (Müller *et al.*, 2004; Caillaud *et al.*, 2008; Smertenko *et al.*, 2008; Ho *et al.*, 2011).

Another discrepancy is the intracellular localization of MAP65-4 reported here and that by previous studies. The overexpressed MAP65-4-GFP fusion protein exclusively labeled perinuclear MTs and kinetochore fibers (Van Damme *et al.*, 2004; Fache *et al.*, 2010), which is different from what is described in the current study. Several lines of evidence would be in favor of the result reported here. First, the MAP65-4-GFP fusion protein was a functional because it rescued the deficiency cause by the loss of MAP65-3; and a similar MAP65-3 fusion protein was already been proven to be functional (Ho *et al.*, 2011). Furthermore, the fusion protein was expressed under its native promoter but not a constitutively active one. Third, the fusion protein was expressed in the genetic background of the *map65-4* null mutation so that the expressed MAP65-4 protein was the only form of the isoform in cells. Lastly, examinations were carried out in meristematic cells in root tips so that they were physiologically unaltered because the transgenic plants showed comparable growth patterns to the wild-type control. We suggest that caution should be particularly exercised in interpreting the localization result when an isoform is expressed at elevated or unregulated levels in a heterologous system.

Nevertheless, our results perhaps represent a vivid example of the acquisition of a new function by an evolutionarily conserved protein such as MAP65-4 while it still moonlights a function normally fulfilled by its ancestral protein of the MAP65/Ase1p family on anti-parallel MTs in cell division.

Cooperative contributions of two MAP65 isoforms to organizing phragmoplast MTs

Given the synthetic lethality of the *map65-3* and *map65-4* mutations, MAP65-3 clearly carries more weight toward organizing phragmoplast MT organization and cytokinesis than MAP65-4 in *A. thaliana*. Homologous cytoskeletal proteins often assume redundant functions as reported in *A. thaliana*. For example, Kinesin-12A and Kinesin-12B play a redundant role in

establishing the minimal MT overlapping zone in the phragmoplast (Lee *et al.*, 2007). Coincidently, similar rules can be applied to the Kinesin-14 motors KIN14a and KIN14b, as well as the Kinesin-7 motors NACK1 and NACK2 (Tanaka *et al.*, 2004; Quan *et al.*, 2008). Other than the redundancy, both pairs of motors also demonstrated unequal functions. For example, loss of KIN14a in the *atk1* mutant causes severe defects in organizing the meiotic spindles in the microsporocytes while the division goes on normally in the absence of KIN14b (Chen *et al.*, 2002; Ambrose & Cyr, 2007). Likewise, the loss of NACK1 in the *hinkel* mutant causes incomplete cytokinesis in somatic tissues while the loss of NACK2 in the *stud* or *tetraspore* mutant causes defects in male meiotic division (Hülskamp *et al.*, 1997; Spielman *et al.*, 1997; Nishihama *et al.*, 2002; Strompen *et al.*, 2002). One may argue that such a phenomenon can be attributed to differential gene expression, as demonstrated by the mitogen-activated protein kinases MPK4 and MPK11, which is perhaps another example of unequal redundancy (Kosetsu *et al.*, 2010). While the *mpk4* mutant shows serious defects in cytokinesis, *mpk11* behaves like the wild-type. Interestingly, MPK11 expression is greatly elevated in the *mpk4* mutant and *mpk11* enhances the growth defect caused by *mpk4* (Kosetsu *et al.*, 2010). To discern such an assumption, it would be informative if experiments similar to those included here are carried out for these kinesins.

Our previous study indicated that a chimera of MAP65-1 with the C-terminal domain of MAP65-3 could accomplish much of the function normally assigned to MAP65-3 while overexpression of MAP65-1 did not (Ho *et al.*, 2012). Our results summarized here further support the notion that the C-terminus of MAP65-4 enables the protein to acquire an overlapping function with MAP65-3 in the phragmoplast. Perhaps this overlapping function is not shared by other MAP65 isoforms. This assumption is based on the data that the *map65-3* (−/−); *map65-1* (−/−) mutant was not only viable but also produced significantly more healthy and robust seedlings than the *map65-3* (−/−); *map65-4* (+/−) mutant. How do the overlapping functions of MAP65-3 and MAP65-4 differentially contribute to phragmoplast MT organization? Our results suggested that MAP65-4 might be a multi-functional MAP65 isoform, based on the cell cycle-dependent localization in meristematic cells. Its function in the phragmoplast perhaps is similar to that of MAP65-3. This statement is supported by the fact that limited success of cytokinesis in the *map65-3* null mutant became sensitive to the dose of the MAP65-4 gene. Furthermore, the addition of an extra copy of *MAP65-4* greatly suppressed the growth defects caused by the *map65-3* null mutation. The emphasized function of MAP65-3 in the phragmoplast could be attributed to the higher expression level of MAP65-3 than that of MAP65-4. Another possibility is that MAP65-3 has a higher affinity to anti-parallel MTs than MAP65-4 during development of the phragmoplast. In the absence of MAP65-3, however, MAP65-4 would have more convenient access to the overlapping zone of the phragmoplast by cross-linking them.

One of the remaining tasks would be to determine how the C-termini of MAP65-3 and MAP65-4 may specify their functions in cytokinesis that are divergent from the rest of the MAP65 isoforms. One likely scenario is that the domains enable their interaction with factors that specifies their action at overlapped MT plus ends in the phragmoplast.

Potential function of MAP65-4 in cell division plane determination

Previously, more than one MAP65 isoform was detected at the PPB by antibody immunolocalization or GFP tagging (Müller *et al.*, 2004; Caillaud *et al.*, 2008; Smertenko *et al.*, 2008; Li *et al.*, 2009). In particular, a GFP-MAP65-2 fusion protein selectively marked the PPB MTs but not those on the nuclear envelope in prophase cells upon overexpression (Li *et al.*, 2009). The significance of the PPB association has not been determined as to date no phenotypes in cell division plane determination have been documented in any *map65* mutant plants. Here we showed that MAP65-4 was not only associated with the PPB but also persisted at the cortical division site after the disappearance/disassembly of the PPB even after cells entered cytokinesis. This type of localization echoes those of proteins important for cell division plane determination (Rasmussen *et al.*, 2013). Among them, the basic protein TAN (Tangled) directly interacts with MTs (Smith *et al.*, 2001). So do two homologous Kinesin-12 proteins, POK1 and POK2, owing to them being MT-based motors. The kinesins interact with TAN directly and are required for persistent appearance of TAN at the cortical division site after PPB disassembly (Lipka *et al.*, 2014). Compared with the weak division plane phenotypes, but not overall plant growth phenotypes, linked to the *tan1* mutation in *A. thaliana*, simultaneous loss of both POK1 and POK2 leads to serious defects in the guidance of the expanding cell plate during cytokinesis, reminiscent of that of the *tangled 1* mutant in maize (Cleary & Smith, 1998; Müller *et al.*, 2006; Walker *et al.*, 2007). Surprisingly, the RanGAP1 protein also behaves as a continuous positive marker at the cortical division site and requires POK1/2 for its retention at the site in *A. thaliana* (Xu *et al.*, 2008). Loss-of-function mutations of these factors could even lead to the appearance of incomplete cell plate stubs due to cytokinesis failures in addition to division plane orientation problems (Xu *et al.*, 2008). However, how these factors function in cell division remains unknown.

Coincidently, the plant-specific Kinesin-14 motor KCBP (Kinesin-like Calmodulin Binding Protein) also remains at the cortical division site after disappearance of the PPB, besides its association with the spindle poles (Buschmann *et al.*, 2015). Similar to the *map65-4* mutant, loss of KCBP in the *zwi* mutant does not cause noticeable defects in cell division either (Oppenheimer *et al.*, 1997). To elucidate the potential function in cell division plane determination as suggested by the localization to the division site, we would have to investigate the genetic interaction between *zwi* and *map65-4* as well as between *tan* and *map65-4* by generating double mutants. Alternatively, potential interactions between MAP65-4 and one or more of these proteins could be informative as well.

Aside from the aforementioned MT-associated factors, in the moss *Physcomitrella patens*, the Myosin VIII motor Myo8A was detected at MT ends in developing phragmoplasts and exhibited

persistent localization at the cortical division site in mitosis and cytokinesis, and the collective function of motors in this subfamily is critical for division plane determination (Wu & Bezanilla, 2014). Therefore, the cortical division site perhaps is where MT-associated factors communicate with those associated with actin microfilaments in order to preserve the division plane established by the PPB at earlier stages of cell division and interpret it at later stages. It is certainly worth testing whether MAP65-4 interacts with the Arabidopsis counterpart(s) of the moss Myo8A once they are identified.

Currently, it is unclear how the redistribution of MAP65-4 is regulated from prophase to cytokinesis. It is puzzling how MAP65 would be able to remain at the cortical division site after the PPB is disassembled. One particular note is that whether MAP65-4 molecules localized to the cortical division site could capture newly polymerized MTs at the expanding edge of the phragmoplast. In fact, such an activity has been demonstrated by MAP65-1 upon overexpression, although not at the cell cortex (Murata *et al.*, 2013). This activity may be related to the connection between the expanding phragmoplast MT array and the cortical division site marked by MAP65-4 during cytokinesis.

Acknowledgements

Author contributions

Y-R.J.L., Y.M. and B.L. planned and designed the research. H. Li, B.S., M.S. X.D. and Y-R.J.L. performed experiments and analysed data. Y-R.J.L., Y.M., H. Lin and B.L. wrote and revised the manuscript.

References

Ambrose JC, Cyr R. 2007. The kinesin ATK5 functions in early spindle assembly in *Arabidopsis*. *Plant Cell* 19: 226–236.

Buschmann H, Dols J, Kopischke S, Pena EJ, Andrade-Navarro MA, Heinlein M, Szymanski DB, Zachgo S, Doonan JH, Lloyd CW. 2015. *Arabidopsis* KCBP interacts with AIR9 but stays in the cortical division zone throughout mitosis via its MyTH4-FERM domain. *Journal of Cell Science* 128: 2033–2046.

Caillaud M-C, Lecomte P, Jammes F, Quentin M, Pagnotta S, Andrio E, de Almeida Engler J, Marfaing N, Gounon P, Abad P et al. 2008. MAP65-3 microtubule-associated protein is essential for nematode-induced giant cell ontogenesis in *Arabidopsis*. *Plant Cell* 19: 423–437.

Chen CB, Marcus A, Li WX, Hu Y, Calzada JPV, Grossniklaus U, Cyr RJ, Ma H. 2002. The Arabidopsis *ATK1* gene is required for spindle morphogenesis in male meiosis. *Development* 129: 2401–2409.

Cleary AL, Smith LG. 1998. The *Tangled1* gene is required for spatial control of cytoskeletal arrays associated with cell division during maize leaf development. *Plant Cell* 10: 1875–1888.

Czechowski T, Stitt M, Altmann T, Udvardi MK, Scheible WR. 2005. Genome-wide identification and testing of superior reference genes for transcript normalization in Arabidopsis. *Plant Physiology* 139: 5–17.

Fache V, Gaillard J, Van Damme D, Geelen D, Neumann E, Stoppin-Mellet V, Vantard M. 2010. *Arabidopsis* kinetochore fiber-associated MAP65-4 cross-links microtubules and promotes microtubule bundle elongation. *Plant Cell* 22: 3804–3815.

Guo L, Ho C-MK, Kong Z, Lee Y-RJ, Qian Q, Liu B. 2009. Evaluating the microtubule cytoskeleton and its interacting proteins in monocots by mining the rice genome. *Annals of Botany* 103: 387–402.

Hamada T. 2014. Microtubule organization and microtubule-associated proteins in plant cells. *International Review of Cell and Molecular Biology* 312: 1–52.

Hamada T, Nagasaki-Takeuchi N, Kato T, Fujiwara M, Sonobe S, Fukao Y, Hashimoto T. 2013. Purification and characterization of novel microtubule-associated proteins from Arabidopsis cell suspension cultures. *Plant Physiology* 163: 1804–1816.

Ho CM, Hotta T, Guo F, Roberson RW, Lee YR, Liu B. 2011. Interaction of antiparallel microtubules in the phragmoplast is mediated by the microtubule-associated protein MAP65-3 in Arabidopsis. *Plant Cell* 23: 2909–2923.

Ho CM, Lee YR, Kiyama LD, Dinesh-Kumar SP, Liu B. 2012. Arabidopsis microtubule-associated protein MAP65-3 cross-links antiparallel microtubules toward their plus ends in the phragmoplast via its distinct C-terminal microtubule binding domain. *Plant Cell* 24: 2071–2085.

Hülskamp M, Parekh N, Grini P, Schneitz K, Zimmermann I, Lolle S, Pruitt R. 1997. The STUD gene is required for male-specific cytokinesis after telophase II of meiosis in *Arabidopsis thaliana*. *Developmental Biology* 187: 114–124.

Jiang CJ, Sonobe S. 1993. Identification and preliminary characterization of a 65-kDa higher-plant microtubule-associated protein. *Journal of Cell Science* 105: 891–901.

Kong Z, Hotta T, Lee YR, Horio T, Liu B. 2010. The γ-tubulin complex protein GCP4 is required for organizing functional microtubule arrays in *Arabidopsis thaliana*. *Plant Cell* 22: 191–204.

Kosetsu K, Matsunaga S, Nakagami H, Colcombet J, Sasabe M, Soyano T, Takahashi Y, Hirt H, Machida Y. 2010. The MAP kinase MPK4 is required for cytokinesis in *Arabidopsis thaliana*. *Plant Cell* 22: 3778–3790.

Lee YR, Li Y, Liu B. 2007. Two Arabidopsis phragmoplast-associated kinesins play a critical role in cytokinesis during male gametogenesis. *Plant Cell* 19: 2595–2605.

Lee YRJ, Liu B. 2000. Identification of a phragmoplast-associated kinesin-related protein in higher plants. *Current Biology* 10: 797–800.

Li H, Zeng X, Liu ZQ, Meng QT, Yuan M, Mao TL. 2009. Arabidopsis microtubule-associated protein AtMAP65-2 acts as a microtubule stabilizer. *Plant Molecular Biology* 69: 313–324.

Lipka E, Gadeyne A, Stockle D, Zimmermann S, De Jaeger G, Ehrhardt DW, Kirik V, Van Damme D, Muller S. 2014. The phragmoplast-orienting Kinesin-12 class proteins translate the positional Information of the preprophase band to establish the cortical division zone in *Arabidopsis thaliana*. *Plant Cell* 26: 2617–2632.

Lucas JR, Courtney S, Hassfurder M, Dhingra S, Bryant A, Shaw SL. 2011. Microtubule-associated proteins MAP65-1 and MAP65-2 positively regulate axial cell growth in etiolated *Arabidopsis* hypocotyls. *Plant Cell* 23: 1889–1903.

Lucas JR, Shaw SL. 2012. MAP65-1 and MAP65-2 promote cell proliferation and axial growth in Arabidopsis roots. *Plant Journal* 71: 454–463.

Mao T, Jin L, Li H, Liu B, Yuan M. 2005. Two microtubule-associated proteins of the Arabidopsis MAP65 family function differently on microtubules. *Plant Physiology* 138: 654–662.

Müller S, Han S, Smith LG. 2006. Two kinesins are involved in the spatial control of cytokinesis in *Arabidopsis thaliana*. *Current Biology* 16: 888–894.

Müller S, Smertenko A, Wagner V, Heinrich M, Hussey P, Hauser M. 2004. The plant microtubule-associated protein AtMAP65-3/PLE is essential for cytokinetic phragmoplast function. *Current Biology* 14: 412–417.

Murata T, Sano T, Sasabe M, Nonaka S, Higashiyama T, Hasezawa S, Machida Y, Hasebe M. 2013. Mechanism of microtubule array expansion in the cytokinetic phragmoplast. *Nature Communications* 4: 1967.

Nakagawa T, Kurose T, Hino T, Tanaka K, Kawamukai M, Niwa Y, Toyooka K, Matsuoka K, Jinbo T, Kimura T. 2007. Development of series of gateway binary vectors, pGWBs, for realizing efficient construction of fusion genes for plant transformation. *Journal of Bioscience and Bioengineering* 104: 34–41.

Nishihama R, Soyano T, Ishikawa M, Araki S, Tanaka H, Asada T, Irie K, Ito M, Terada M, Banno H *et al.* 2002. Expansion of the cell plate in plant cytokinesis requires a kinesin-like protein/MAPKKK complex. *Cell* 109: 87–99.

Oppenheimer DG, Pollock MA, Vacik J, Szymanski DB, Ericson B, Feldmann K, Marks MD. 1997. Essential role of a kinesin-like protein in Arabidopsis trichome morphogenesis. *Proceedings of the National Academy of Sciences, USA* 94: 6261–6266.

Pfaffl MW. 2001. A new mathematical model for relative quantification in real-time RT-PCR. *Nucleic Acids Research* 29: e45.

Quan L, Xiao R, Li W, Oh SA, Kong H, Ambrose JC, Malcos JL, Cyr R, Twell D, Ma H. 2008. Functional divergence of the duplicated *AtKIN14a* and *AtKIN14b* genes: critical roles in Arabidopsis meiosis and gametophyte development. *Plant Journal* 53: 1013–1026.

Rasmussen CG, Wright AJ, Muller S. 2013. The role of the cytoskeleton and associated proteins in determination of the plant cell division plane. *Plant Journal* 75: 258–269.

Sasabe M, Kosetsu K, Hidaka M, Murase A, Machida Y. 2011. *Arabidopsis thaliana* MAP65-1 and MAP65-2 function redundantly with MAP65-3/ PLEIADE in cytokinesis downstream of MPK4. *Plant Signaling & Behavior* 6: 743–747.

Sasabe M, Soyano T, Takahashi Y, Sonobe S, Igarashi H, Itoh TJ, Hidaka M, Machida Y. 2006. Phosphorylation of NtMAP65-1 by a MAP kinase down-regulates its activity of microtubule bundling and stimulates progression of cytokinesis of tobacco cells. *Genes & Development* 20: 1004–1014.

Smekalova V, Luptovciak I, Komis G, Samajova O, Ovecka M, Doskocilova A, Takac T, Vadovic P, Novak O, Pechan T *et al.* 2014. Involvement of YODA and mitogen activated protein kinase 6 in Arabidopsis post-embryogenic root development through auxin up-regulation and cell division plane orientation. *New Phytologist* 203: 1175–1193.

Smertenko AP, Chang HY, Sonobe S, Fenyk SI, Weingartner M, Bogre L, Hussey PJ. 2006. Control of the AtMAP65-1 interaction with microtubules through the cell cycle. *Journal of Cell Science* 119: 3227–3237.

Smertenko AP, Kaloriti D, Chang HY, Fiserova J, Opatrny Z, Hussey PJ. 2008. The C-terminal variable region specifies the dynamic properties of Arabidopsis microtubule-associated protein MAP65 isotypes. *Plant Cell* 20: 3346–3358.

Smith LG, Gerttula SM, Han SC, Levy J. 2001. TANGLED1: a microtubule binding protein required for the spatial control of cytokinesis in maize. *Journal of Cell Biology* 152: 231–236.

Spielman M, Preuss D, Li F, Browne W, Scott R, Dickinson H. 1997. TETRASPORE is required for male meiotic cytokinesis in *Arabidopsis thaliana*. *Development* 124: 2645–2657.

Strompen G, El Kasmi F, Richter S, Lukowitz W, Assaad FF, Jurgens G, Mayer U. 2002. The Arabidopsis HINKEL gene encodes a kinesin-related protein involved in cytokinesis and is expressed in a cell cycle-dependent manner. *Current Biology* 12: 153–158.

Tanaka H, Ishikawa M, Kitamura S, Takahashi Y, Soyano T, Machida C, Machida Y. 2004. The *AtNACK1/HINKEL* and *STUD/TETRASPORE/ AtNACK2* genes, which encode functionally redundant kinesins, are essential for cytokinesis in *Arabidopsis*. *Genes to Cells* 9: 1199–1211.

Van Damme D, Van Poucke K, Boutant E, Ritzenthaler C, Inze D, Geelen D. 2004. *In vivo* dynamics and differential microtubule-binding activities of MAP65 proteins. *Plant Physiology* 136: 3956–3967.

Walczak CE, Shaw SL. 2010. A MAP for bundling microtubules. *Cell* 142: 364–367.

Walker KL, Muller S, Moss D, Ehrhardt DW, Smith LG. 2007. *Arabidopsis* TANGLED identifies the division plane throughout mitosis and cytokinesis. *Current Biology* 17: 1827–1836.

Wu SZ, Bezanilla M. 2014. Myosin VIII associates with microtubule ends and together with actin plays a role in guiding plant cell division. *eLife* 3: e03498.

Xu XM, Zhao Q, Rodrigo-Peiris T, Brkljacic J, He CS, Muller S, Meier I. 2008. RanGAP1 is a continuous marker of the Arabidopsis cell division plane. *Proceedings of the National Academy of Sciences, USA* 105: 18637–18642.

Supporting Information

Additional Supporting Information may be found online in the Supporting Information tab for this article:

Fig. S1 Sequence alignment of *Arabidopsis thaliana* MAP65-1, MAP65-3 and MAP65-4 by Clustal Omega (http://www.ebi.ac.uk/Tools/msa/clustalo/).

Fig. S2 Comparison of growth of various *map65* mutant plants in *Arabidopsis thaliana* using the wild-type as the control after growing for 60 d.

Fig. S3 Rescue of the *map65-3/ map65-3*; *map65-4/ map65-4* double mutant by MAP65-4-GFP expression in *Arabidopsis thaliana*.

Fig. S4 Suppression of the cytokinesis defect caused by the *map65-3* mutation in *Arabidopsis thaliana*.

Fig. S5 Comparison of the expression levels of AtMAP65-4 mRNA in *Arabidopsis thaliana* by quantitative real-time RT-PCR.

Fig. S6 MAP65-3 localization in the *map65-4* mutant cells in *Arabidopsis thaliana*.

Please note: Wiley Blackwell are not responsible for the content or functionality of any Supporting Information supplied by the authors. Any queries (other than missing material) should be directed to the *New Phytologist* Central Office.